Nonlinear dc transport in graphene

2009 J. Phys.: Condens. Matter 21 305302

(http://iopscience.iop.org/0953-8984/21/30/305302)

J. Phys.: Condens. Matter **21** (2009) 305302 (5pp) doi:10.1088/0953-8984/21/30/305302

Nonlinear dc transport in graphene

W S Bao[1], S Y Liu[1], X L Lei[1] and C M Wang[2]

[1] Department of Physics, Shanghai Jiaotong University, 800 Dongchuan Road, Shanghai 200240, People's Republic of China
[2] Department of Physics, Anyang Normal University, Anyang 455000, People's Republic of China

E-mail: liusy@sjtu.edu.cn

Received 17 February 2009, in final form 24 June 2009
Published 8 July 2009
Online at stacks.iop.org/JPhysCM/21/305302

Abstract

Considering electron–impurity, electron–acoustic-phonon and electron–optical-phonon scatterings, the nonlinear steady-state transport properties of graphene are studied theoretically by means of the balance equation approach. We find that the conductivity as a function of electric field strength, E, exhibits strongly nonlinear behavior for E larger than a critical value, $E_c \approx 0.1$ kV cm^{-1}. With the increase of E from zero, the conductivity first decreases slowly and then it falls rapidly when $E > E_c$. The dependence of electron temperature on E is also demonstrated.

(Some figures in this article are in colour only in the electronic version)

1. Introduction

Recently, graphene, a single-atom-thick two-dimensional (2D) layer of carbon atoms in a hexagonal honey-combed lattice composed of two superposed triangular sub-lattices, has attracted a great deal of theoretical and experimental attention [1–5]. In this 2D system, the energy of carriers in the vicinity of two nodal ('Dirac') points of the Brillouin zone linearly depends on the carrier momentum and the low-energy carriers behave as massless, two-dimensional, relativistic fermions [6–8]. Such an unusual electronic structure leads to many interesting phenomena, including high mobility at room temperature, finite residual conductivity in the limit of vanishing carrier density [1, 9], the room-temperature quantum Hall effect [10], etc. Graphene also has great potential applications in industry. To date, applications of graphene as graphene-based chemical sensors [11], spin-valve devices [12], electromechanical resonators [13], etc have been demonstrated.

In the first experiment involving graphene, a finite 'residual' conductivity, $\sigma_{res} \approx 4e^2/h$, in the carrier density dependence of conductivity at zero gate voltage was observed. This unusual transport property stimulates an extensively theoretical investigation on the linear transport in graphene. Much theoretical effort has been devoted to the quantitative explanation of the observed σ_{res} [14–33]. However, the issue has been confused with the findings of various values of residual conductivity by using different theoretical approaches. For relatively high electron density, the conductivity σ in graphene was found to be proportional to the charge density N as $\sigma \approx 20(e^2/h)(N/n_i)$ (n_i is the impurity density) [26, 28]. In the presence of only electron–acoustic-phonon scattering, the linear transport properties in high-electron-density graphene have also been investigated [34]. It was found that the resistivity ρ is proportional to T at relative high temperature, while ρ varies as T^4 at low temperature.

In this paper, we investigate the nonlinear dc transport properties of graphene by means of the balance equation approach, considering electron–impurity, electron–acoustic-phonon, and electron–optical-phonon scatterings. To our knowledge, the transport of graphene driven by a strong dc electric field has only been studied by Akturka and Goldsman using the Monte-Carlo method [35]. The balance equation approach, which includes force- and energy-balance equations, has been proven to be useful and convenient for studying steady-state high-field transport in semiconductors [36–38]. Applying this method to a graphene system, we find that a strong nonlinear effect in the dependence of conductivity on the electric field strength, E, appears when E is larger than a critical value E_c of about 0.1 kV cm^{-1}. The conductivity decreases slowly with an increase of E from zero to E_c while it falls rapidly with a further increase of E. We also find that, at low lattice temperature, electron temperature T_e sharply increases to 300–400 K when E increases. This effect comes from the fact that the electron–optical-phonon scattering, which provides an effective energy dissipation channel, is important only for $T_e > 300$ K.

This paper is organized as follows. In section 2, the balance equation approach in the graphene system is presented. The numerical investigation on the nonlinear transport in graphene is shown in section 3. Finally, the results are concluded in section 4.

2. Balance equations in graphene

We consider a single-layer graphene in the x-y plane driven by an in-plane strong uniform dc electric field, $\boldsymbol{E}$. In this system, there are two valleys in the first Brillouin zone. Near each valley, the wavefunction of an electron with momentum $\boldsymbol{k} = (k_x, k_y) = (k\cos\phi_k, k\sin\phi_k)$ ($k = |\boldsymbol{k}|$ is the magnitude of $\boldsymbol{k}$ and $\phi_k = \arctan(k_y/k_x)$ is its polar angle) can be written as [39]

$$|\boldsymbol{k}\rangle = \frac{1}{\sqrt{2}}\begin{pmatrix} 1 \\ \mathrm{e}^{\mathrm{i}\phi_k} \end{pmatrix}, \tag{1}$$

and the dispersion relation of energy takes the form

$$\varepsilon(\boldsymbol{k}) = \hbar v_{\mathrm{F}}|\boldsymbol{k}| = \hbar v_{\mathrm{F}} k, \tag{2}$$

with v_{F} as the Fermi velocity. Apparently, both valleys make the same contributions to the transport. Hence, we neglected the valley index for simplicity.

In the present paper, we will use the balance equation approach to investigate the dc nonlinear transport in graphene. The balance equation approach is one of the most powerful tools for studying the nonlinear transport in semiconductors. It separates the center-of-mass motion from the relative motion of the many-electron system and the system can be described by single particle energy bands. The electron–electron interactions, in addition to their role in promoting the thermalization, are taken into account mainly as the screening (for a review, see [37]). For simplicity we will take only static screening into consideration.

In the balance equation approach, the transport properties of electrons in an arbitrary energy band are described by the lattice momentum shift $\boldsymbol{p}_d$, electron temperature T_{e}, and chemical potential μ. These parameters are determined by the force- and energy-balance equations taking the forms [38]

$$e\boldsymbol{E}\cdot\mathcal{K} + \boldsymbol{a}_{\mathrm{i}} + \boldsymbol{a}_p = 0, \tag{3}$$

$$e\boldsymbol{E}\cdot\boldsymbol{v}_d - w = 0, \tag{4}$$

with

$$\boldsymbol{v}_d = \langle\hat{\boldsymbol{v}}\rangle = \frac{g_{\mathrm{s}}g_{\mathrm{v}}}{N}\sum_{\boldsymbol{k}}\boldsymbol{v}(\boldsymbol{k})\, f(\bar{\varepsilon}(\boldsymbol{k}), T_{\mathrm{e}}) \tag{5}$$

as the drift velocity, and

$$\mathcal{K} = \frac{g_{\mathrm{s}}g_{\mathrm{v}}}{N}\sum_{\boldsymbol{k}}\frac{1}{\hbar^2}\nabla_{\boldsymbol{k}}\nabla_{\boldsymbol{k}}\varepsilon(\boldsymbol{k})\, f(\bar{\varepsilon}(\boldsymbol{k}), T_{\mathrm{e}}) \tag{6}$$

as the ensemble-averaged inverse effective mass tensor. $f(\bar{\varepsilon}(\boldsymbol{k}), T_{\mathrm{e}}) = \{\exp[(\bar{\varepsilon}(\boldsymbol{k}) - \mu)/(k_{\mathrm{B}}T_{\mathrm{e}})] + 1\}^{-1}$ [$\bar{\varepsilon}(\boldsymbol{k}) = \varepsilon(\boldsymbol{k} - \boldsymbol{p}_d)$] is the displaced Fermi distribution function of electrons driven by a strong dc field. It relates to the total number of electrons N by

$$N = g_{\mathrm{s}}g_{\mathrm{v}}\sum_{\boldsymbol{k}} f(\bar{\varepsilon}(\boldsymbol{k}), T_{\mathrm{e}}), \tag{7}$$

with $g_{\mathrm{s}} = 2$ and $g_{\mathrm{v}} = 2$ as the spin and valley degeneracies, respectively. In equations (3) and (4), $\boldsymbol{a}_{\mathrm{i}}$ is the acceleration due to electron–impurity scattering, while $\boldsymbol{a}_p$ and w are, respectively, the acceleration and energy dissipation rate arising from electron–phonon interaction.

In 2D gated graphene, the main electron–impurity scattering comes from ionized dopants within a narrow space charge layer with total area density n_{i} at a distance d from the interface in the substrate side. This scattering can be described by a potential $u(q)$ of the form

$$u(q) = \frac{v(q,d)}{\epsilon(q)}, \tag{8}$$

with $v(q,d) = e^2\exp(-qd)/(2\epsilon_0\kappa q)$ as unscreened electron–impurity scattering potential and κ as the effective background lattice dielectric constant depending on the substrate material. $\epsilon(q)$ is the 2D static dielectric (screening) function due to electron–electron interaction. Within the random phase approximation it can be written as [40]

$$\epsilon(q) = 1 + \frac{q_{\mathrm{s}}}{q}\begin{cases} 1 & q \leqslant 2k_{\mathrm{F}} \\ 1 + \dfrac{\pi q}{8k_{\mathrm{F}}} - \dfrac{\sqrt{q^2 - 4k_{\mathrm{F}}}}{2q} & \\ \quad -q\dfrac{2\sin^{-1}(2k_{\mathrm{F}}/q) - \pi}{8k_{\mathrm{F}}} & q > 2k_{\mathrm{F}} \end{cases} \tag{9}$$

with $q_{\mathrm{s}} = e^2k_{\mathrm{F}}/(\pi\epsilon_0\hbar\kappa v_{\mathrm{F}}) = 4k_{\mathrm{F}}r_{\mathrm{s}}$ as the effective Thomas–Fermi wavevector in 2D graphene. Such $u(q)$ leads to $\boldsymbol{a}_{\mathrm{i}}$ of the form

$$\begin{aligned}\boldsymbol{a}_{\mathrm{i}} = {} & \frac{g_{\mathrm{s}}g_{\mathrm{v}}\pi n_{\mathrm{i}}}{N\hbar}\sum_{\boldsymbol{k},\boldsymbol{q}}|u(q)|^2|g(\boldsymbol{k},\boldsymbol{q})|^2 \\ & \times[\boldsymbol{v}(\boldsymbol{k}+\boldsymbol{q}) - \boldsymbol{v}(\boldsymbol{k})]\delta(\varepsilon(\boldsymbol{k}+\boldsymbol{q}) - \varepsilon(\boldsymbol{k})) \\ & \times[f(\bar{\varepsilon}(\boldsymbol{k}), T_{\mathrm{e}}) - f(\bar{\varepsilon}(\boldsymbol{k}+\boldsymbol{q}), T_{\mathrm{e}})],\end{aligned} \tag{10}$$

with $g(\boldsymbol{k},\boldsymbol{q})$ as the form factor relating to the electron wavefunction by

$$g(\boldsymbol{k},\boldsymbol{q}) = \langle\boldsymbol{k}+\boldsymbol{q}|\boldsymbol{k}\rangle = \tfrac{1}{2}(1 + \mathrm{e}^{\mathrm{i}(\phi_k - \phi_{k+q})}). \tag{11}$$

In graphene, we also need to consider the deformation-potential interactions between electrons and phonons including longitudinal acoustic and optical branches. The corresponding scattering matrix elements of these interactions can be written as [34, 35]

$$|M(\boldsymbol{q},\alpha)|^2 = \frac{D^2\hbar Q_\alpha^2}{2A\rho_{\mathrm{m}}\Omega_{q,\alpha}}, \tag{12}$$

with D as the deformation-potential coupling constant, ρ_{m} as the graphene mass density, A as the area of the sample, and $\Omega_{q,\alpha}$ as the frequency of the αth branch phonon with wavevector $\boldsymbol{q}$. Q_α depends on the phonon modes: $Q_\alpha = q$ for acoustic phonon and $Q_\alpha = 2\pi/a$ for optical phonon (a is the lattice constant). Within the framework of the balance equation approach, the electron–phonon scattering leads to the acceleration and energy dissipation rate, $\boldsymbol{a}_p$ and w, which take

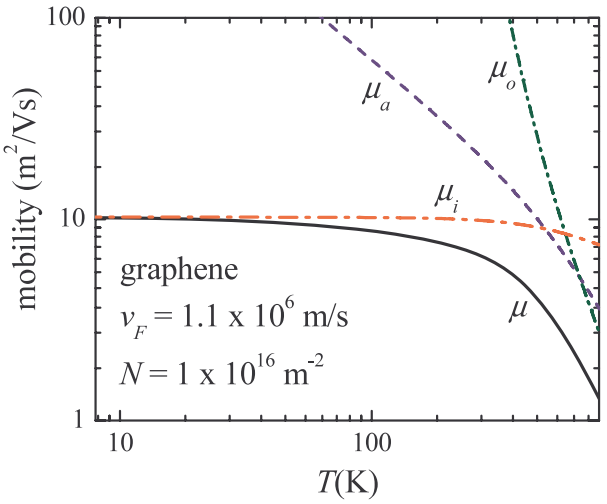

Figure 1. Dependencies of total mobility μ, impurity-limited mobility $\mu_{\rm i}$, acoustic-phonon-limited mobility $\mu_{\rm a}$, and optical-phonon-limited mobility $\mu_{\rm o}$ on the lattice temperature.

the forms

$$a_p = \frac{2g_{\rm s}g_{\rm v}\pi}{N\hbar}\sum_{k,q,\alpha}|M(q,\alpha)|^2|g(k,q)|^2[v(k+q) - v(k)]\delta(\varepsilon(k+q)-\varepsilon(k)+\hbar\Omega_{q,\alpha}) \times [f(\bar{\varepsilon}(k),T_{\rm e}) - f(\bar{\varepsilon}(k+q),T_{\rm e})] \times \left[n\left(\frac{\hbar\Omega_{q,\alpha}}{k_{\rm B}T}\right) - n\left(\frac{\bar{\varepsilon}(k)-\bar{\varepsilon}(k+q)}{k_{\rm B}T_{\rm e}}\right)\right], \quad (13)$$

$$w = \frac{2g_{\rm s}g_{\rm v}\pi}{N\hbar}\sum_{k,q,\alpha}|M(q,\alpha)|^2|g(k,q)|^2\hbar\Omega_{q,\alpha} \times \delta(\varepsilon(k+q)-\varepsilon(k)+\hbar\Omega_{q,\alpha}) \times [f(\bar{\varepsilon}(k),T_{\rm e}) - f(\bar{\varepsilon}(k+q),T_{\rm e})] \times \left[n\left(\frac{\hbar\Omega_{q,\alpha}}{k_{\rm B}T}\right) - n\left(\frac{\bar{\varepsilon}(k)-\bar{\varepsilon}(k+q)}{k_{\rm B}T_{\rm e}}\right)\right]. \quad (14)$$

In these equations, T is the lattice temperature and $n(x) = (e^x - 1)^{-1}$ is the Bose function.

3. Numerical results

Solving the balance equations, (3) and (4), we perform a numerical investigation on the nonlinear transport properties of graphene. In the calculation, the frequency of longitudinal optical (LO) phonon, $\Omega_{q,\rm LO} \equiv \Omega_{\rm LO}$, is assumed to be independent of the momentum q and its value is chosen to be $\Omega_{\rm LO} = 298.3$ THz [41]. The frequency of the longitudinal acoustic (LA) phonon is linear in q: $\Omega_{q,\rm LA} \equiv v_{\rm sl}q$, with $v_{\rm sl}$ as the longitudinal sound velocity. In typical graphene, $v_{\rm sl} = 2.0 \times 10^4$ m s^{-1} [42, 43]. The other parameters used in the calculation are $a = 2.45$ Å, $D = 19.0$ eV, $\rho_{\rm m} = 7.6 \times 10^{-7}$ kg m^{-2}, $\kappa = 2.5$ [26, 34], and $v_{\rm F} = 1.1 \times 10^6$ m s^{-1} [3]. The impurity density $n_{\rm i}$ is determined by zero-temperature mobility, which is fixed at 10 m^2 V s^{-1}. The distance between the layers of impurities and electrons is $d = 0.1$ nm. The dependencies of calculated conductivity, $\sigma \equiv v_d/E$, and electron temperature $T_{\rm e}$ on the lattice temperature T and/or electric field E are plotted in figures 1–3.

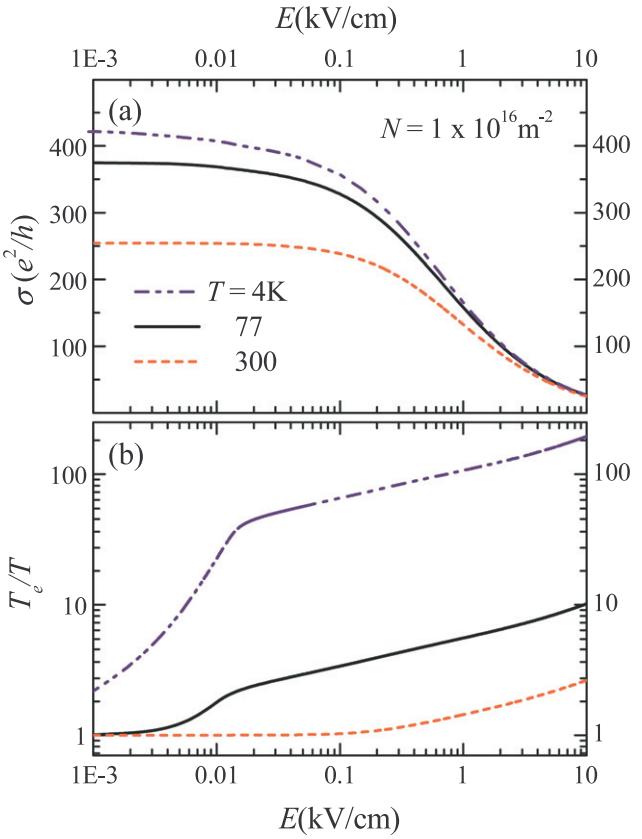

Figure 2. Dependencies of conductivity σ and electron temperature $T_{\rm e}$ on the strength of external electric field E at various lattice temperatures T.

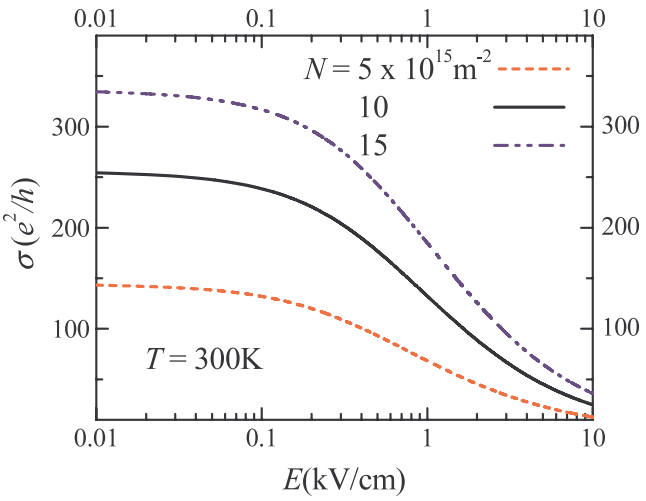

Figure 3. The conductivity σ as a function of electric field E in graphene with various carrier densities N at $T = 300$ K.

3.1. The linear case

In the limit of weak electric field, the inverse of total mobility, $1/\mu[\mu \equiv \sigma/(Ne)]$, is the sum of impurity contribution $1/\mu_{\rm i}$, acoustic-phonon contribution $1/\mu_{\rm a}$, and optical-phonon contribution $1/\mu_{\rm o}$:

$$\frac{1}{\mu} = \frac{1}{\mu_{\rm i}} + \frac{1}{\mu_{\rm a}} + \frac{1}{\mu_{\rm o}}. \quad (15)$$

The dependencies of these quantities on temperature in graphene with the electron density $N = 1 \times 10^{16}$ m^{-2} are shown in figure 1. We see that, at temperature less than 20 K, the contributions to $1/\mu$ from electron–phonon scattering (both from the electron–acoustic-phonon and electron–optical-phonon interactions) are less than 3%, and the impurity scattering dominates the electron transport. With the increase of temperature, the electron–phonon scattering becomes more influential. When the temperature goes up as high as 300–400 K, the effect of phonon scattering is comparable with that of impurity scattering. As temperature reaches more than about 700 K, the optical-phonon scattering is dominant in the contribution to $1/\mu$.

It is noted that the linear transport properties of graphene for $d = 0$ at zero temperature can be carried out analytically within the balance equation approach. In this case, $a_i \approx \frac{\partial a_i}{\partial p_d}|_{p_d=0} \cdot p_d$ and $a_p = 0$. Substituting them into equation (3), we can obtain $p_d = \frac{eE}{\pi\hbar} \cdot \frac{k_F}{v_F} \cdot \frac{1}{G(2r_s)n_i}$, with $G(x) = \frac{x^2}{16}\int_0^{2\pi} \frac{\sin^2\theta}{(\sin\frac{\theta}{2}+x)^2}\mathrm{d}\theta$. Hence, the drift velocity takes the form

$$v_d \approx \left.\frac{\partial v_d}{\partial p_d}\right|_{p_d=0} \cdot p_d = \frac{eE}{\pi\hbar} \cdot \frac{1}{G(2r_s)n_i}, \tag{16}$$

and the conductivity can be written as

$$\sigma = \frac{Nev_d}{E} = \frac{2}{G(2r_s)}\frac{e^2}{h}\frac{N}{n_i}. \tag{17}$$

For the chosen parameters, $r_s \approx 0.8$, $G(2r_s) \approx 0.1$ and hence $\sigma = 20\frac{e^2}{h}\frac{N}{n_i}$, agreeing with [26, 28].

3.2. The nonlinear case

Further, we perform a numerical investigation on the nonlinear transport in graphene. The results are shown in figures 2 and 3. In all these plotted results, the maximum strength of the electric field we consider is 10 kV cm^{-1} because graphene breaks down under laser electric fields of 20 kV cm^{-1} (10^6 W cm^{-2} of power). In figure 2(a), conductivity σ versus the electric field E at various lattice temperatures T is shown. We see that, when $E \lesssim 0.1$ kV cm^{-1}, the conductivity remains practically unchanged with the increase of E. This is associated with the fact that, for such low E, the electron–impurity scattering plays a dominant role. As E becomes higher than 0.1–1 kV cm^{-1}, σ declines evidently due to the increase of electron–acoustic-phonon scattering. In this case, the optical-phonon scattering as a dissipation mechanism also indirectly limits the further increase of drift velocity by influencing electron temperature T_e. In figure 2(b), the quantities of ratio T_e/T are plotted as a function of the electric field E at various lattice temperatures. At $T = 300$ K, T_e is approximately equal to the lattice temperature until E increases to a value higher than 0.1 kV cm^{-1}. At $T = 77$ K, an apparent ascending T_e/T comes out when E goes up to 3×10^{-3} kV cm^{-1}. At $T = 4$ K, T_e/T increases evidently when the strength of the electric field is enhanced higher than 10^{-4} kV cm^{-1}. When T_e rises up to some critical point, 300–400 K, for all the cases above, the rate of increment of T_e/T with respect to the electric field slows down since, at such T_e, the electron–optical-phonon scattering plays an important role in energy dissipation, limiting the increase rate of electron temperature.

In figure 3, conductivities versus the external electric field E at room temperature 300 K are plotted for various electron densities. It is clear that the conductivity σ is almost independent of E for $E \lesssim 0.1$ kV cm^{-1} since the electron–impurity scattering dominates. However, with an increase of E, the impact of phonon scattering is more and more effective in suppressing the electron drift velocity, making the conductivity decline and approach zero. It is noted that the graphene system with higher carrier density always has lower resistivity.

4. Conclusions

Considering electron–impurity, election-acoustic-phonon, and electron–optical-phonon, the transport properties of graphene driven by a strong dc electric field have been studied by means of the balance equation approach. It was found that with an increase in the strength of electric field, conductivity versus E shows strongly nonlinear behavior for E larger than the critical value $E_c \approx 0.1$ kV cm^{-1}: the conductivity decreases slowly for $E < E_c$ while it falls rapidly for $E > E_c$. We have also found that with the increase of E, the electron temperature sharply increases to 300–400 K, at which, the optical-phonon scattering effectively dissipates the energy coming from the electric field.

Acknowledgments

This work was supported by the projects of the National Science Foundation of China and the Shanghai Municipal Commission of Science and Technology, and from the Program for New Century Excellent Talents in University.

References

[1] Novoselov K S, Geim A K, Morozov S V, Jiang D, Zhang Y, Dubonos S V, Grigorieva I V and Firsov A A 2004 *Science* **306** 666
[2] Novoselov K S, Geim A K, Morozov S V, Jiang D, Katsnelson M I, Grigorieva I V, Dubonos S V and Firsov A A 2005 *Nature* **438** 197
[3] Zhang Y, Small J P, Amori M E S and Kim P 2005 *Phys. Rev. Lett.* **94** 176803
[4] Zhang Y, Tan Y-W, Stormer H L and Kim P 2005 *Nature* **438** 201
[5] For recent reviews see e.g. Katsnelson M L 2006 *Mater. Today* **10** 20
Castro Neto A H, Guinea F, Peres N M R, Novoselov K S and Geim A K 2009 *Rev. Mod. Phys.* **81** 109
[6] Wallace P R 1947 *Phy. Rev.* **71** 622
[7] Semenoff G W 1984 *Phys. Rev. Lett.* **53** 2449
[8] Haldane F D M 1988 *Phys. Rev. Lett.* **61** 2015
[9] Berger C, Song Z, Li X, Wu X, Brown N, Naud C, Mayou D, Li T, Hass J, Machenkov A N, Conrad E H, First P N and de Heer W A 2006 *Science* **312** 1191
[10] Novoselov K S, Jiang Z, Zhang Y, Morozov S V, Stormer H L, Zeitler U, Maan J C, Boebinger G S, Kim P and Geim A K 2007 *Science* **315** 1379
[11] Schedin F, Geim A K, Morozov S V, Hill E W, Blake P, Katsnelson M I and Novoselov K S 2007 *Nat. Mater.* **6** 652

[12] Hill E W, Geim A K, Novoselov K S, Schedin F and Blake P 2006 *IEEE Trans. Magn.* **42** 2694
[13] Bunch J S, van der Zande A M, Verbridge S S, Frank I W, Tanenbaum D M, Parpia J M, Craighead H G and McEuen P L 2007 *Science* **315** 490
[14] Fradkin E 1986 *Phys. Rev.* B **33** 3263
[15] Lee P A 1993 *Phys. Rev. Lett.* **71** 1887
[16] Gorbar E V, Gusynin V P, Miransky V A and Shovkovy I A 2002 *Phys. Rev.* B **66** 045108
[17] Ludwig A W W, Fisher M P A, Shankar R and Grinstein G 1994 *Phys. Rev.* B **50** 7526
[18] Gusynin V P and Sharapov S G 2005 *Phys. Rev. Lett.* **95** 146801
[19] Peres N M R, Guinea F and Castro Neto A H 2006 *Phys. Rev.* B **73** 125411
[20] Katsnelson M I 2006 *Eur. Phys. J.* B **51** 157
[21] Tworzydlo J, Trauzettel B, Titov M, Rycerz A and Beenakker C W J 2006 *Phys. Rev. Lett.* **96** 246802
[22] Ziegler K 2006 *Phys. Rev. Lett.* **97** 266802
[23] Falkovsky L A and Varlamov A A 2007 *Eur. Phys. J.* B **56** 281
[24] Ziegler K 2007 *Phys. Rev.* B **75** 233407
[25] Nomura K and MacDonald A H 2007 *Phys. Rev. Lett.* **98** 076602
[26] Adam S, Hwang E H, Galitski V and Das Sarma S 2007 *Proc. Natl Acad. Sci. USA* **104** 18392
[27] Galitski V M, Adam S and Das Sarma S 2007 *Phys. Rev.* B **76** 245405
[28] Hwang E H, Adam S and Das Sarma S 2007 *Phys. Rev. Lett.* **98** 186806
[29] Auslender M and Katsnelson M I 2007 *Phys. Rev.* B **76** 235425
[30] Trushin M and Schliemann J 2007 *Phys. Rev. Lett.* **99** 216602
[31] Liu S Y, Lei X L and Horing N J M 2008 *J. Appl. Phys.* **104** 043705
[32] Lherbier A, Blase X, Niquet Y-M, Triozon F and Roche S 2008 *Phys. Rev. Lett.* **101** 036808
[33] Yan X-Z, Romiah Y and Ting C S 2008 *Phys. Rev.* B **77** 125409
[34] Hwang E H and Das Sarma S 2008 *Phys. Rev.* B **77** 115449
[35] Akturka A and Goldsman N 2008 *J. Appl. Phys.* **103** 053702
[36] Lei X L and Ting C S 1984 *Phys. Rev.* B **30** 4809
Lei X L and Ting C S 1985 *Phys. Rev.* B **32** 1112
[37] Lei X L and Horing N J M 1992 *Int. J. Mod. Phys.* B **6** 805
[38] Lei X L, Horing N J M and Cui H L 1991 *Phys. Rev. Lett.* **66** 3227
Lei X L 1992 *Phys. Status Solidi* **170** 519
[39] Nomura K and MacDonald A H 2007 *Phys. Rev. Lett.* **98** 076602
[40] Hwang E H and Das Sarma S 2007 *Phys. Rev.* B **75** 205418
[41] Maultzsch J, Reich S, Thomsen C, Requardt H and Ordejón P 2004 *Phys. Rev. Lett.* **92** 075501
[42] Pietronero L, Strässler S, Zeller H R and Rice M J 1980 *Phys. Rev.* B **22** 904
Woods L M and Mahan G D 2000 *Phys. Rev.* B **61** 10651
Suzuura H and Ando T 2002 *Phys. Rev.* B **65** 235412
Pennington G and Goldsman N 2003 *Phys. Rev.* B **68** 045426
[43] Ono S and Sugihara K 1966 *J. Phys. Soc. Japan* **21** 861
Sugihara K 1983 *Phys. Rev.* B **28** 2157